express
polymer letters

Research article

Coordination crosslinks of epoxidized natural rubber with reactive zinc chloride

Kamonthip Rittimas[ID]*, Skulrat Pichaiyut*[ID]*, Charoen Nakason**[ID]

Faculty of Science and Industrial Technology, Surat Thani Campus, Prince of Songkla University, 84000 Surat Thani, Thailand

Abstract. Epoxidized natural rubber with 50 mol% epoxide (ENR-50) was compounded with zinc chloride ($ZnCl_2$) and subjected to torque response analysis using a moving die rheometer. It was found that different $ZnCl_2$ concentrations (3, 5, 7, 9, and 12 millimoles (mmol)) mixed in ENR-50 exhibited positive torque responses, prompting further molecular characterization using Fourier transform infrared spectroscopy. The results indicated distinct absorption peaks at wavenumbers of 442 and 809 cm^{-1}, which signify the presence of –O–Zn–O– coordination linkages. The curing characteristics of ENR and $ZnCl_2$ compounds showed that increasing $ZnCl_2$ content resulted in higher minimum and maximum torque values, but also led to a decrease in scorch time and cure rate index (*CRI*). Moreover, higher $ZnCl_2$ concentrations enhanced the strength properties (tensile strength, moduli, stiffness, toughness, and hardness), crosslink densities, dynamic shear moduli, initial modulus during relaxation experiments, and thermal resistance, as evidenced by temperature scanning stress relaxation (TSSR), thermogravimetric analysis, and dynamic mechanical analysis. However, an increase in $ZnCl_2$ content led to a reduction in elongation at break due to the higher crosslink density within the coordination networks in the ENR matrix, which resulted in the movement constraint of the rubber vulcanizate.

Keywords: epoxidized natural rubber (ENR), zinc chloride, coordination reaction, internal polymerization, thermo-mechanical properties

1. Introduction

Natural rubber (NR) is one of the most important elastomeric materials in industrial applications that cannot be replaced by synthetic counterparts in many important applications. This is owing to its unique excellent properties, including mechanical, dynamic, and damping properties [1], as well as resilience, elasticity, abrasion and impact resistance, efficient heat dispersion, and malleability at low temperatures. Consequently, natural rubber has found unique applications in heavily loaded tires, aircraft tires, surgical gloves, medical devices, anti-vibration products, and countless other engineering and consumer products [2]. However, molecular chains in natural rubber abundantly contain unsaturation, which limits certain industrial applications due to its poor thermal, aging, and oil-resistant properties [3]. One approach to diminish or suppress this limitation is to modify the NR molecular chains, for instance, by incorporating some reactive functional groups into NR molecules. There have been varieties of modified NR alternatives, including epoxidized natural rubber (ENR), maleated natural rubber (MNR), and grafted copolymers of NR with various vinyl monomers [4]. However, the most frequently used modified NR is epoxidized natural rubber (ENR), with epoxide or oxirane polar functional groups. ENRs have been commercially produced, such as Epoxyprene 25 (ENR-25) and Epoxyprene 50 (ENR-50), indicating 25 and 50% epoxidation, respectively. For instance,

---

these types of rubbers are manufactured by Muang Mai Guthrie Public Company Limited, located in Surat Thani, Thailand [5]. ENR typically exhibits properties resembling those of synthetic rubbers in terms of good oil resistance [6], air permeability [7], as well as strength properties [8]. Also, ENR is still capable of undergoing strain crystallization since oxygen is small enough to fit into the crystal lattice with only minor geometrical rearrangements [8]. Typically, prior to achieving qualified performance with high dimensional stability in various rubber applications, crosslinking among rubber molecules is necessarily commenced through various vulcanization or crosslinking systems. This affects the creation of crosslinking structures where the linear macromolecules of elastomeric material convert to stronger, along with a permanent rubber vulcanizate consisting of a three-dimensional crosslinked network. Therefore, the basis of vulcanization is the creation of chemical crosslinks between rubber macromolecules, which leads to the formation of a three-dimensional network, through chemical reactions between the reactive functional groups in elastomeric chains and suitable curing agents [9]. Sulfur vulcanization is the oldest process used in the crosslinking of unsaturated elastomers and is one of the most important curing systems for NR and its derivatives. Typically, sulfur curing systems consist of at least three ingredients: sulfur, activators, and accelerators. These components lead to the creation of sulfidic crosslinks of varying lengths, including one, two, or multiple sulfidic linkages (*i.e.*, monosulfidic, disulfidic, and polysulfidic) between rubber molecular chains [10]. However, there are other potential vulcanization systems for crosslinking rubber molecules, including peroxide [9, 11], phenolic resin [12], dicarboxylic [13], and imidazole [14] curing systems. These curing systems typically create various covalently bonded crosslinked network types, including a group of sulfur atoms in a short chain, a single sulfur atom, carbon-to-carbon bonds, as well as links among polar atoms [15]. However, other types of bonds involving metal atoms have also been developed, such as ionic clusters and polyvalent metal ion links [15]. In such cases, for instance, a metal compound mixture of zinc oxide (ZnO) and $ZnCl_2$ could accelerate the vulcanization of chlorinated poly(isoprene-co-isobutylene) (CIIR or chloro-butyl rubber) [16]. Additionally, magnesium oxide (MgO) could create ionic crosslinks in carboxylated nitrile rubber [17].

In general, the incorporation of metal ions into reactive polymer molecules with polar functionality can cause the formation of complexes through coordination reactions between transition metal ions and ligands [18]. These reactions also lead to the formation of strong three-dimensional network structures of rubber molecules, which, in some instances, can cause reversible changes both at normal and high temperatures [19]. In addition, various types of metal ions have been exploited to cure different types of polar rubber through coordination linkages. For instance, coordination crosslinking networks can be formed based on Nitrile butadiene rubber (NBR)/$ZnCl_2$ composites, which result from the coordination reaction between zinc ions (Zn^{2+}) and nitrile groups in NBR molecules [20]. High polarity rubbers like acrylate rubber (AR) can undergo a crosslinking reaction through coordination bonds between the ester groups in acrylate rubber and cupric ions (Cu^{2+}) present in inorganic metal salts such as copper sulfate ($CuSO_4$) [21]. This type of coordination-bonded network could occur more favorably at room temperature, with a higher rate if the reaction temperature is raised. Furthermore, the extent of crosslinking, crosslinking density, and tensile strength increased with increasing loading of $CuSO_4$ and curing temperature [21]. In addition, carboxylated nitrile rubber (XNBR) was also coordination crosslinked by reacting between Cu^{2+} within anhydrous copper sulfate ($CuSO_4$) and the nitrile ($–C≡N$) groups, along with the formation of ionic bonds between copper ions and carboxylic groups in XNBR molecules [22]. In addition, a self-healing XNBR rubber was prepared based on the metal-ligand coordination between the 2,6-diaminopyridine (DAP) ligand and different metal ions (Co^{2+}, Ni^{2+}, and Zn^{2+}) moieties attached to the XNBR backbone [23].

In natural rubber containing polar functional groups such as ENR, coordination crosslinking is favored by reacting the polar functional epoxirane groups or their ring-opened products with different types of metal ions. For instance, the coordination reaction between ENR and stannous dichloride ($SnCl_2·2H_2O$) has been investigated, revealing the formation of an ENR and stannous (Sn) coordination (ENR/Sn) complex wherein stannous dichloride molecules are inserted into the quaternary and methine carbon atoms [24]. In this circumstance, Fourier-transform infrared spectroscopy (FTIR) and proton nuclear magnetic resonance (NMR) confirmed the formation

of a four-coordinated Sn complex, while transmission electron microscopy (TEM) analysis revealed a ring-coil shape with a thick lining [32]. Additionally, ferric ions were introduced into an oxygen-abundant commercially available rubber network using epoxidized natural rubber and ferric chloride ($FeCl_3$) or ENR-$FeCl_3$ model compounds. This resulted in the formation of additional metal-oxygen coordination crosslinks via complexation, which influenced the enhancement of strength, toughness, and damping properties [25]. Additionally, the crosslinking reaction of epoxidized natural rubber with 50 mol% epoxide (ENR-50) with ferric ions (Fe^{3+}) from ferric chloride ($FeCl_3$) has been investigated, as described in our previous work [26]. This investigation revealed that the Fe^{3+} ion could interact with the hydroxyl groups from the opened oxirane ring products of ENR to create new –O–Fe–O– linkages between ENR molecular chains via the alpha (α) and beta (β) carbon atoms. Moreover, another type of reaction, called internal polymerization reaction, simultaneously occurred during the mixing of ENR-50 and Fe^{3+} [26, 27]. Increasing concentrations of $FeCl_3$ resulted in an increase in the crossinking density, moduli, and strength [26]. Furthermore, carbon nanotubes (CNTs) filled ENR with coordination and internal polymerization reactions with Fe^{3+}, resulting in outstanding mechanical and electrical characteristics. For instance, enhancements were observed in the torque difference, modulus, tensile strength, and electrical conductivity with increasing CNT loadings [27]. Similar phenomena were observed in ENR-50-filled hybrid fillers containing both CNTs and conductive carbon black (CCB) [28]. Furthermore, the metal-ligand coordination between ENR and $FeCl_3$ could enhance the self-healing performance of ENR compounds [29]. Moreover, an ionic and coordination hybrid network in a self-healing elastomer was formed from the reaction of ENR with Zn^{2+} metal ions and 2-aminopyridine (AP) grafted onto ENR as the ligand, creating coordination and ionic bonds to construct the hybrid network [30]. Furthermore, Zn-containing zeolitic imidazolate, based on zinc ions coordinating with different imidazolate ligands, was added to natural rubber (NR). It was found that the addition of zeolitic imidazolate facilitated faster vulcanization of NR at lower cure temperatures [31]. Therefore, among different types of metal ions, zinc (II) ions may be one of the potential crosslinking agents for polar natural rubber-like ENR.

In this study, we undertook preliminary research on the coordination reactions of ENR-50 with varying concentrations of zinc chloride via a dry mixing process. Firstly, we observed torque responses during the curing test using the rotorless moving die rheometer (MDR) at 160 °C. Infrared spectroscopy was then employed to verify the newly formed chemical linkages in the epoxidized natural rubber and zinc chloride (ENR-$ZnCl_2$) compounds, elucidating the proposed reaction mechanism. Furthermore, we conducted various comparative analyses, including assessments of curing, mechanical, dynamic, thermal, thermos-mechanical, and electrical properties of ENR compounds. Our primary objective was to investigate the potential coordination reaction between $ZnCl_2$ and ENR-50, aiming to develop a novel vulcanization system for natural rubber and advance the field of self-healing rubber products.

2. Experimental
2.1. Materials
Epoxidized natural rubber with 50±2 mol% epoxide (ENR-50) was obtained from Muangmai Guthrie Co., Ltd., located in Surat Thani province, Thailand. ENR-50 has a Mooney viscosity, ML(1+4) at 100 °C, in the range of 70–100 units, along with an ash content of less than 0.5 wt%. Reagent-grade zinc chloride ($ZnCl_2$), used for coordination with ENR-50, was obtained from Sigma-Aldrich, located in Darmstadt, Germany. Toluene, used in the swelling experiment for the determination of the crosslink density of the ENR vulcanizate, was produced by Carlo Erba Reagents S.A.S., located in De Rueil, France.

2.2. Preparation of ENR-50 compounded with zinc chloride
ENR-50 (58.0 g) was first dried in a hot air oven at 60 °C for approximately 24 h. It was then mixed with various concentrations of $ZnCl_2$ at 3, 5, 7, 9, and 12 mmol using the Brabender measuring mixer, model 50 EHT, manufactured by Brabender Plasticorder located in Duisburg, Germany. It is noted that the weight equivalents of different concentrations at 3, 5, 7, 9, and 12 mmol are 0.43, 0.72, 1.00, 1.29, and 1.71 g, respectively. The initial temperature for mixing was set at 60 °C with a rotation velocity of rotors at 60 rpm. The ENR was masticated for approximately 3 min before adding the zinc chloride compound into the mixing chamber, followed by an additional 8 min of mixing. The rubber compound

was then removed from the mixing chamber and conditioned at room temperature for at least 1 h. Next, the rubber sheet was fabricated by passing it through a 1 mm nip of an open two-roll mill, model YFCR 600, from Yong Fong Machinery Co., Ltd., located in Samut Sakorn province, Thailand, at ambient temperature. The ENR-ZnCl$_2$ rubber sheet was subsequently conditioned in a desiccator at room temperature for about 24 h. The torque response was then investigated at 160 °C using a rotorless moving die rheometer, MDR 2000, from Alpha Technologies, located in Hudson, USA. After observing a positive torque response due to coordination crosslinking, the vulcanized rubber sheets were fabricated by compression molding. This was done using a PR1D-W400L450PM molding machine from Charon Tut Co., Ltd., located in Samut Sakorn province, Thailand, at 160 °C and a compression pressure of about 700 kPa, maintaining the respective cure times as determined by the moving die rheometer (MDR) test.

2.3. Determination of coordination crosslinking and curing characteristic

The torque response was utilized to monitor the existence of coordination and other related reactions between ENR-50 and ZnCl$_2$. Moreover, for the positive torque response, the curing characteristics of the ENR-ZnCl$_2$ compounds were evaluated following the standard ISO 6502. This was conducted using a moving die rheometer, model MDR 2000, from Alpha Technologies, located in Hudson, USA. The analysis was carried out at a constant oscillation frequency of 1.67 Hz and a strain amplitude of 1°, maintained at 160 °C. This testing procedure generated the torque-time relationships, or curing curves, for different ENR-ZnCl$_2$ compounds, which allowed for the determination of various significant curing parameters. These parameters encompass scorch time (t_{s2}), cure time (t_{c90}), minimum torque (M_L), maximum torque (M_H), torque difference ($M_H - M_L$), and the reaction rate represented by the cure rate index (*CRI*). It is noted that the optimum cure time (t_{c90}) is the time required for the torque to reach 90% of the maximum achievable torque and indicates the time necessary for the cured rubber to achieve its optimum properties.

2.4. Infrared spectroscopy

FTIR was utilized to analyze neat ENR-50 along with various ENR-ZnCl$_2$ compounds with different concentrations of ZnCl$_2$ (3, 5, 7, 9, and 12 mmol) in the transmission mode using a Spectrum Two FT-IR Spectrometer with a deuterated triglycine sulfate (DTGS) detector, manufactured by PerkinElmer, Inc., located in Waltham, USA. Thin sheets of rubber specimens with smooth surfaces were initially fabricated and subsequently subjected to structural analysis by being placed in the attenuated total reflectance (ATR) device of FT-IR for solid contact sampling. The FTIR analysis was then conducted, covering a broad wavenumber range from 4000 to 400 cm^{-1} and at a resolution of 4 cm^{-1}.

2.5. Mechanical properties

Tensile test specimens were initially prepared by mechanically die-cutting from the previously prepared rubber vulcanizate sheets, following ISO 37 standards. Subsequently, these samples were placed within the sample holder of a tensile testing machine sourced from Tinus Olsen Ltd, located in Honey Crock Lane, UK. The tensile tests were then carried out at ambient temperature, with extension occurring at a crosshead speed of 200 mm/min, in accordance with ISO 37 guidelines. Additionally, the hardness property of various rubber specimens was evaluated using a Shore A durometer, model HT 3000 SA by Montech, based in Buchen, Germany, following the standard procedure outlined in ISO 868.

2.6. Crosslink density

A swelling experiment was conducted to ascertain the crosslink density of rectangular rubber specimens measuring 10×10×2 mm. Initially, the weight of the rubber samples was recorded prior to immersion in toluene at room temperature for seven days in the dark. Subsequently, the swollen rubber samples were removed, and any excess liquid on the specimen surfaces was eliminated using filter paper. Following this, the specimens were dried in a vacuum oven at 40 °C for 24 h. Finally, the original weight was compared with the final weight before and after immersion in toluene. The crosslink density of the rubber vulcanizates was determined utilizing the Flory–Rehner relation, Equation (1) [32]:

$$\nu = \frac{\ln(1 - \phi_p) + \chi \cdot \phi_p^2}{V_L \left(\phi_p^{1/3} - \frac{\phi_p}{2} \right)} \qquad (1)$$

where ϕ_π is the volume fraction of rubber in the swollen network, V_L is the molar volume of toluene and χ is the interaction parameter of polymer and solvent (for ENR and toluene, the value is 0.34) [33].

2.7. Dynamic mechanical properties

The dynamic mechanical properties of pure ENR-50 and ENR-ZnCl$_2$ compounds were evaluated by measuring the storage modulus (G') and loss tangent ($\tan\delta$) in relation to strain amplitude. This was accomplished using a rubber process analyzer (RPA), specifically the RPA 2000 from Alpha Technologies (Ohio, USA). The test involved measuring the storage shear modulus (G') and $\tan\delta$ of each rubber specimen subjected to shear deformation, with strain amplitude ranging from 0.56 to 100%, at a fixed frequency of 1.0 Hz and a temperature of 100 °C.

2.8. Thermo-mechanical properties

Thermo-mechanical properties during relaxation experiments were monitored through temperature scanning stress relaxation (TSSR) measurements of rubber specimens using a TSSR meter from Brabender Messtechnik® GmbH & Co. KG (Duisburg, Germany). Dumbbell-shaped specimens (type 5A), as per ISO 527 standard, were initially prepared and annealed in a hot air oven at 100 °C for about 30 min to eliminate the thermal history and storage hardening of natural rubber before the TSSR test [34]. Afterward, they were cooled to room temperature and left to rest for around 30 min before initiating the tests. The specimens were stretched up to 50% of their original length and conditioned at 23 °C for approximately 2 h to eliminate short-term relaxation of rubber molecules [35]. Following this, a non-isothermal condition was applied by increasing the temperature from 23 to 220 °C or until the specimen ruptured, using a constant heating rate of 2 °C/min. The stress (or modulus) at each relaxation temperature was then recorded and reported in terms of the relationship between relaxation stress (or modulus) and the tested temperature [42].

2.9. Thermal properties

Two different approaches were employed to characterize the thermal characteristics of ENR-50 and ENR-ZnCl$_2$ compounds, namely dynamic mechanical analysis (DMA), and thermogravimetric analysis (TGA). In DMA, the analysis was conducted using DMA 8000 from Perkin Elmer Inc. (Waltham, MA, USA) in tension mode over a temperature range of –100 to 100 °C, with a heating rate of 3 °C/min and a fixed deformation frequency of 1 Hz. On the other hand, TGA, the thermal stability of neat ENR-50 and ENR-ZnCl$_2$ compounds was evaluated using a thermogravimetric analyzer, TGA-SDTA 851 from Mettler Toledo (Zurich, Switzerland). Measurements were carried out under a nitrogen atmosphere within the temperature range of 30–600 °C, using a heating rate of 10 °C/min.

2.10. Electrical properties

The electrical properties, specifically electrical conductivity (σ) and dielectric constant (ε'), of pure ENR-50 and ENR-ZnCl$_2$ compounds, were assessed at room temperature using an LCR meter, model IM 3533, manufactured by Hioki E.E. Corporation (Nagano, Japan), across frequency ranges from 1 to 10^5 Hz. The LCR meter was connected to the electrode plates of a dielectric test fixture, model 16451B, from Test Equipment Solutions Ltd. (Berkshire, UK), featuring electrode plates with a diameter of 5 mm. The electrical conductivity (σ) and dielectric constant (ε') were determined using the Equations (2) and (3) relations [36, 37]:

$$\sigma = \frac{1}{\rho} = \frac{d}{R_p \cdot A} \qquad (2)$$

$$\varepsilon' = \frac{C_p \cdot d}{A \cdot \varepsilon_0} \qquad (3)$$

where, d and A represent the sample thickness and the area of an electrode, respectively. The parameter ε_0 denotes the dielectric constant of free space, which is $8.854 \cdot 10^{-12}$ F/m and C_p is the capacity of the capacitor.. The factor ρ signifies the volume resistivity, which is the reciprocal of conductivity.

3. Results and discussion

3.1. Crosslinking reaction and curing properties of ENR-50 compounded with ZnCl$_2$

After ENR-50 was compounded with zinc chloride (ZnCl$_2$) and a positive torque response was observed, a rotorless moving die rheometer, the MDR 2000 manufactured by Alpha Technologies in Ohio, USA, was further utilized to characterize the curing
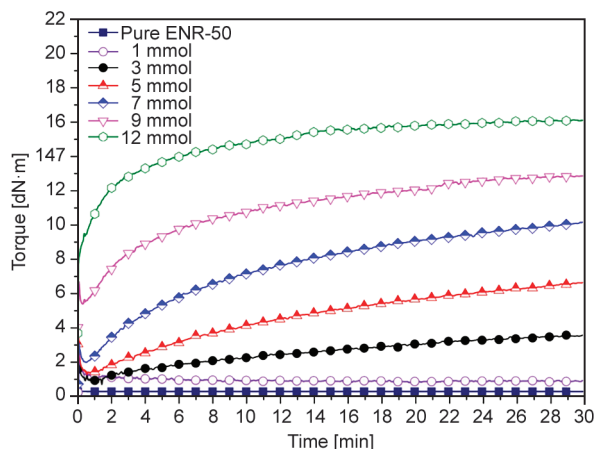
Figure 1. Torque-time curves comparing ENR-50 compounded with various concentrations of ZnCl$_2$ (1, 3, 5, 7, 9, and 12 mmol) to pure ENR-50.

properties of the ENR-ZnCl$_2$ compounds by operating at 160 °C for a duration of 30 min. The resulting torque-time relations are presented in Figure 1. It can be seen that a marginal increasing trend in torque was observed for the ENR compound containing 3 mmol of ZnCl$_2$. In contrast, no torque response was observed for pure ENR-50 or for the sample consisting of 1 mmol of ZnCl$_2$, indicating the absence of reaction among the ENR molecular chains. Furthermore, strong increasing trends in torque were clearly demonstrated with increasing concentrations of ZnCl$_2$ from 5 to 12 mmol. This analysis reveals the typical cure curves, or torque-time curves, for a conventional rubber compound. Initially, there is a sharp drop in torque after the initial rotation of the MDR, followed by a gradual rise to reach the minimum torque (M_L) at the lowest point of the curve. Subsequently, a gradual increase in torque occurs

until reaching the maximum torque value (M_H) around the 15 min mark, specifically for ENR-50 compounded with 12 mmol ZnCl$_2$, while the others demonstrate slightly increasing torque with time-lapse or marching cure curves. It is noteworthy to mention that higher concentrations of ZnCl$_2$ result in a less steep gradient in the torque-time curve, approaching the equilibrium curing curve, as observed in the case of ENR compounded with 12 mmol ZnCl$_2$.

Based on the positive torque responses observed in the torque-time relations in Figure 1, it is evident that the crosslinking reaction between ENR-50 molecules, assisted by ZnCl$_2$, occurred during testing at high temperatures. This assertion is supported by the examination of the molecular structure of ENR networks after the MDR test using ATR-FT-IR, as depicted in Figure 2. In this context, Figure 2a displays the FT-IR spectra covering the entire range of wavenumbers from 4000 to 400 cm^{-1}, while Figure 2b provides a closer view specifically within the wavenumber range of 1200 to 400 cm^{-1}. It can be seen the presence of absorption bands at 1240 and 870 cm^{-1} (Figure 2a) typically refer to symmetric and asymmetric deformations of the epoxy rings in ENR molecules, respectively [38]. Comparison with neat ENR-50 reveals distinct infrared absorption peaks in ENR-ZnCl$_2$ compounds at wavenumbers of 442 and 809 cm^{-1} (Figure 2b), indicating the presence of –O–Zn–O- coordination bonds [39] linking ENR molecules. Additionally, new absorption bands at 1538 cm^{-1} correspond to –C–O stretching vibration [40] in the network structure of ENR crosslinked by Zn^{2+} ions. Moreover, the new absorption
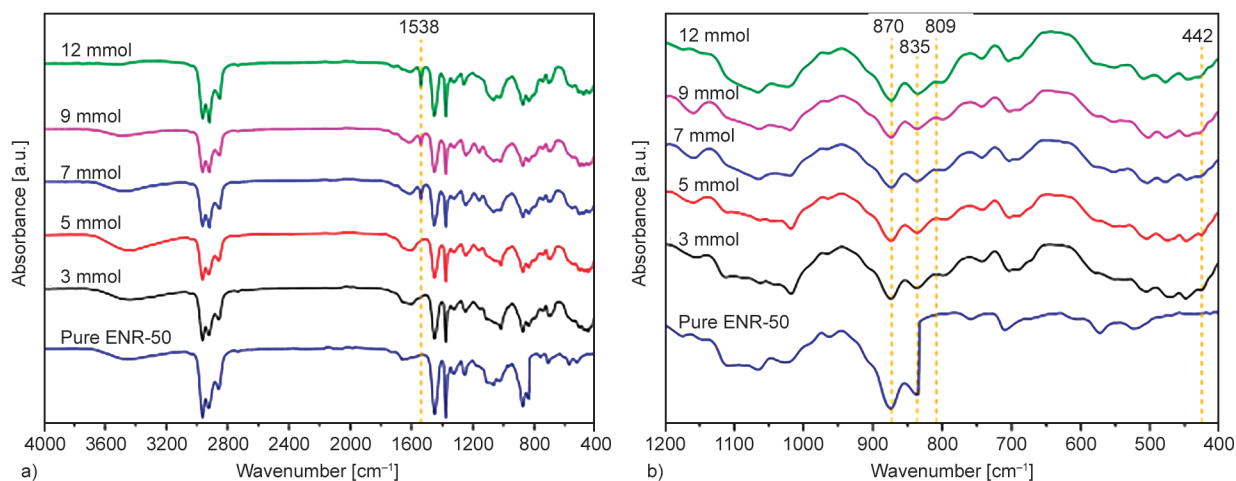
Figure 2. ATR-FTIR spectra of the neat ENR-50 and ENR-50 compounded with 7 mmol ZnCl$_2$. a) In the wavenumber range of 400–4000 cm^{-1}, b) in the wavenumber range of 400–1200 cm^{-1}.
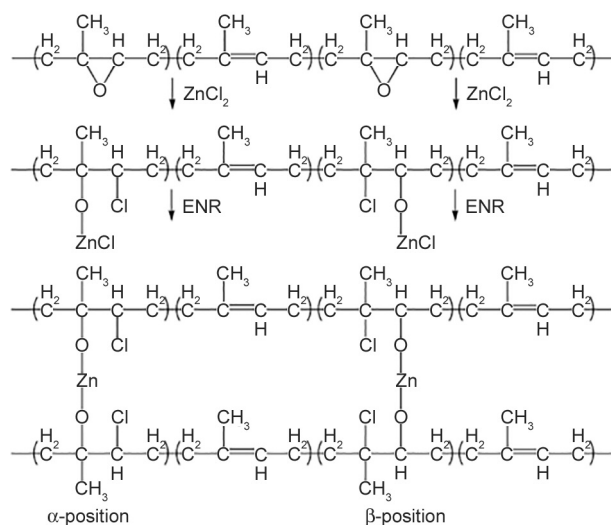
Figure 3. Proposed coordination reaction between ENR-50 and ZnCl$_2$, resulting in the formation of cross-linked rubber networks via complexation at the α and β-carbon atoms of the polyisoprene backbone.

Table 1. Cure characteristics in terms of minimum torque (M_L), maximum torque (M_H), torque difference ($M_H - M_L$), scorch time (t_{s2}), cure time (t_{c90}), cure rate index (*CRI*) of ENR-ZnCl$_2$ compounds with various concentrations of ZnCl$_2$ at 3, 5, 7, 9 and 12 mmol.

ZnCl$_2$ [mmol]	M_L [dN·m]	M_H [dN·m]	$M_H - M_L$ [dN·m]	t_{s2} [min]	t_{c90} [min]	*CRI*
3	1.33	3.58	2.25	1.36	3.35	50.25
5	1.43	6.64	5.21	1.17	6.11	20.24
7	2.02	10.16	8.14	0.75	9.34	11.64
9	5.21	13.21	8.00	0.51	12.11	8.62
12	8.12	16.11	7.99	0.46	15.31	6.73

in ENR-ZnCl$_2$ compounds at a wavenumber of 745 cm^{-1}, which indicates the C–Cl vibration of C–Cl bonds [41, 42], appeared in Figure 2b. Therefore, reactions between ENR-50 and ZnCl$_2$ are proposed, as depicted in Figure 3.

Under elevated temperature and high shear conditions, the oxirane rings within ENR molecules undergo a ring-opening reaction, yielding open-ring products [43]. These adducts with hydroxyl-terminated groups can react with Zn^{2+} ions, forming new linkages connecting ENR molecular chains via the zinc central atom (–O–Zn–O–). In Figure 3, it is also anticipated that the nucleophilic chloride ions could attach to two carbon positions, namely the α-carbon and β-carbon positions in ENR molecules relative to the methyl groups. However, the microstructure at the α-carbon atoms is more reactive due to the presence of a methyl group, imparting a less nucleophilic character to the adjacent carbon atom [44]. This may enhance the likelihood of nucleophilic attack by chloride ions on the carbon atom lacking the methyl groups. The epoxide rings, when exposed to metal ions like Fe^{3+} ions, undergo an internal polymerization reaction [34, 44].

Following the proven evidence of intermolecular crosslinks via the bridge consisting of zinc atoms (–O–Zn–O–), the curing characteristics of different ENR-ZnCl$_2$ compounds were analyzed. Table 1 provides an overview of the curing properties of ENR-50 compounded with varying concentrations of ZnCl$_2$, detailing time and torque-related characteristics. The data display a noticeable trend: as the concentrations

of ZnCl$_2$ increase, both minimum and maximum torque values rise. However, the torque difference, or delta torque, follows an increasing trend until it peaks at a ZnCl$_2$ concentration of 7 mmol before declining. This pattern indicates the level of crosslinking structures within the rubber molecules, reflecting the extent of coordination reaction to create –O–Zn–O– bridges between rubber molecules (as illustrated in Figure 3) alongside the internal polymerization of ENR molecules, both facilitated by the addition of zinc chloride.

In Table 1, a slight decreasing trend in scorch time is observed with increasing ZnCl$_2$ contents, indicating a shorter period during which a rubber compound can be safely processed at a given temperature before curing. This suggests a more rapid reaction at the early stage of the crosslinking process with larger amounts of ZnCl$_2$ present, leading to a rapid onset of the vulcanization process at the beginning of mixing. Conversely, the curing period required to achieve a fully vulcanized rubber network was prolonged with increasing concentrations of ZnCl$_2$ in ENR-50. This phenomenon arises from the fact that higher amounts of ZnCl$_2$ are involved in a higher degree of coordination and internal polymerization reactions to form a denser rubbery network, as evidenced by the magnitude of delta torque. However, when more chloride ions are present than the optimum content of zinc chloride at 7 mmol, they play a more significant role in retarding these reactions [34]. This is correlated with the decreasing trend of the cure rate index (*CRI*), as demonstrated in Table 1.

3.2. Mechanical properties

Figure 4 illustrates the stress-strain behaviors of ENR-ZnCl$_2$ compounds with varying concentrations of ZnCl$_2$, ranging from 3 to 12 mmol. It is evident
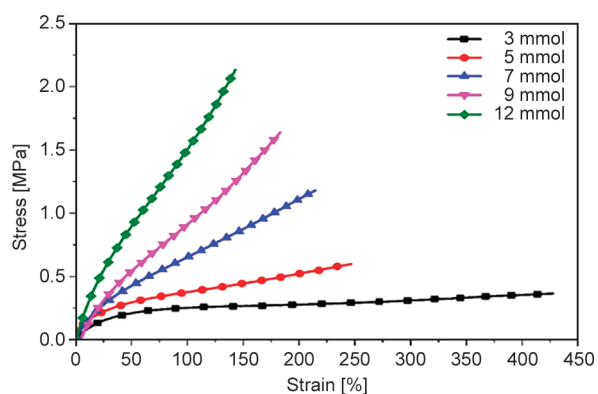
Figure 4. Stress-strain characteristics of ENR-50 compounded with various concentrations (3, 5, 7, 9, and 12 mmol) of $ZnCl_2$.

Figure 5. Crosslinking densities of ENR-50 compounded with $ZnCl_2$ at various concentrations of 3, 5, 7, 9 and 12 mmol.

that the different levels of $ZnCl_2$ loading impact various characteristics under tension stress. Specifically, there is a discernible increase in Young's modulus, reflecting the elastic modulus, with the rise in $ZnCl_2$ concentration within the ENR compounds. It is noted that Young's modulus can be quantified by examining the slopes of the stress-strain curve within the linear elastic region, where stress (force per unit area) is directly proportional to strain (proportional deformation) [45]. Moreover, the elastic modulus serves as a relative measure of a material's stiffness [46]. Consequently, the escalation in $ZnCl_2$ content within ENR-$ZnCl_2$ compounds leads to an increase in elastic modulus and, consequently, the stiffness of the ENR vulcanizate. This observation aligns well with the corresponding increase in hardness, as depicted in Table 2. Additionally, the heightened $ZnCl_2$ content also amplifies the area under the stress-strain relationship, indicating an enhancement in the toughness of the rubber compound [47]. Thus, the augmentation in $ZnCl_2$ content results in elevated elastic moduli, stiffness, and toughness of the ENR vulcanizates, facilitated by the higher coordination reaction

Table 2. Mechanical properties in terms of modulus at 100% elongation, tensile strength, elongation at break, and hardness of ENR 50 compounded with $ZnCl_2$ with various concentrations of 3, 5, 7, 9, and 12 mmol.

$ZnCl_2$ [mmol]	Tensile strength [MPa]	Elongation at break [%]	Modulus at 100% [MPa]	Hardness [Shore A]
3	0.36±0.02	427.4±7.7	0.254±0.03	29.47±1.47
5	0.61±0.08	261.6±4.7	0.378±0.10	33.97±1.69
7	1.18±0.02	215.0±1.2	0.655±1.10	39.60±1.98
9	1.64±0.12	183.3±8.6	0.912±2.31	43.87±2.19
12	2.13±0.02	143.0±6.4	1.533±2.67	48.67±2.43

and internal polymerization of ENR-50 with reactive $ZnCl_2$ compounds.

In Table 2 and Figure 4, there is observable evidence that the increase in $ZnCl_2$ contents influences a corresponding rise in the tensile strength, aligning with the previously mentioned improved physical properties, including stiffness, hardness, as well as toughness. Conversely, the escalation in $ZnCl_2$ content leads to a decrease in the elongation at break or failure strain. This phenomenon can be attributed to a higher degree of crosslinking reactions based on coordination reaction (Figure 3) and internal polymerization, resulting in a higher crosslink density of the rubbery network structures, as depicted in Figure 5. As a consequence, these highly crosslinked structures require more force or stress to undergo shorter or limited elongation before eventual breakage or failure.

3.3. Dynamic mechanical properties
The dynamic mechanical properties of the ENR-$ZnCl_2$ compound were characterized under dynamic shear conditions at 100 °C by RPA, employing a constant oscillating frequency of 1 Hz, coupled with a sweep strain amplitude ranging from 0.56 to 100%. Figure 6 illustrates the range of storage shear modulus (G')-strain magnitude relationships of ENR-$ZnCl_2$ compounds with varying concentrations of $ZnCl_2$. It is clearly seen that strain hardening becomes evident at deformation in the low-strain regime, particularly below 5% strain. This phenomenon is likely attributable to the behavior of the ENR-$ZnCl_2$ compound, as depicted by the marching cure curves (Figure 1), where the ENR compounds still have opportunities for further crosslinking during
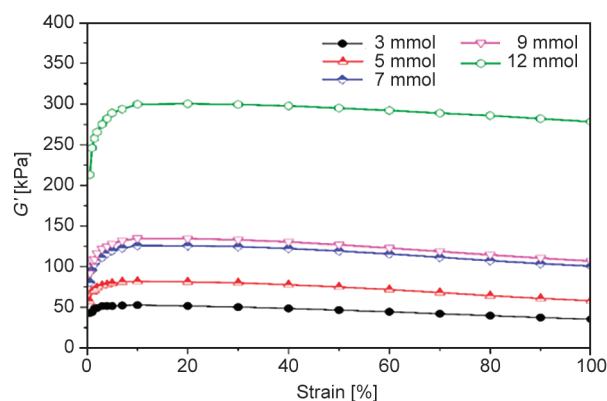
Figure 6. Storage shear modulus-strain amplitude relation-
ships for ENR-50 compounded with varying con-
centrations of $ZnCl_2$ at 3, 5, 7, 9, and 12 mmol.

prolonged curing at high temperatures. Notably, ma-
terials with higher concentrations of $ZnCl_2$ demon-
strate a wider length of this strain range, correlating
with an extended curing time (as indicated in
Table 1) when $ZnCl_2$ content increases in the ENR
compound. Following the initial low-strain regime,
the storage shear modulus tends to decrease upon
achieving full vulcanization of ENR, as evidenced
by the strain-softening regions. This decline can be
attributed to the deterioration of some crosslinks or
other weak bonds due to shear deformation under
high heat conditions. In Figure 6, when considering
the storage modulus-strain amplitude curves, it is ev-
ident that the curve rises higher with increasing con-
tent of $ZnCl_2$ in the ENR compound. This is due to
the enhanced crosslinking reaction facilitated by co-
ordination (as depicted in Figure 3) and internal
polymerization reactions, consequently leading to a
higher crosslinking density (as shown in Figure 6).
This correlation aligns well with the strength prop-
erties observed in Figure 4 and Table 2.
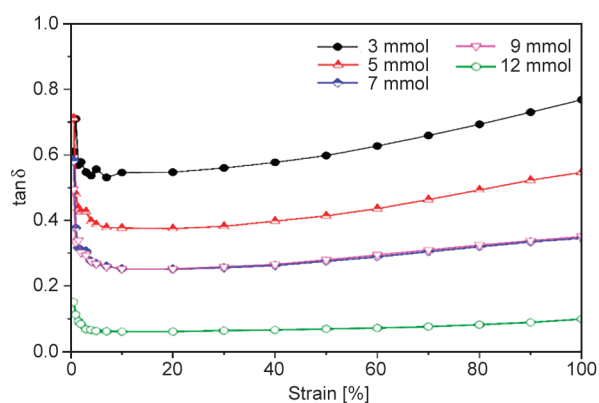
Figure 7 depicts the $\tan\delta$-strain amplitude rela-
tionships for ENR-50 compounded with varying
concentrations of $ZnCl_2$ at 3, 5, 7, 9, and 12 mmol. It
is noted that $\tan\delta$ represents the ratio of the viscous
(G'') to elastic response (G') of a viscoelastic mate-
rial, such as rubber in this study. Therefore, a lower
$\tan\delta$ value indicates a higher elastic response, as ob-
served in the results of this work where $\tan\delta$ values
are below 1.0, indicating a high elasticity of the ma-
terial resulting from these reactions. Furthermore,
during the further crosslinking reaction at the low
strain regimes to form more and stronger ENR net-
works via -O–Zn–O- coordination bonds, the $\tan\delta$
gradually decreases due to gaining more elastic re-
sponse until fully formed networks are created. Sub-
sequently, as described in Figure 6, the $\tan\delta$ gradu-
ally increases due to the rising trend of viscous
response resulting from the breakage of chemical
bonds in the ENR networks. Additionally, it is elab-
orated that the level of $\tan\delta$ at a given strain magni-
tude decreases with increasing $ZnCl_2$ in ENR-$ZnCl_2$
compounds because a stronger crosslinking structure
is formed to gain a more elastic response and hence
a higher elastic nature for the ENR vulcanizate.

3.4. Thermo-mechanical characteristics
Thermo-mechanical analysis of ENR-$ZnCl_2$ com-
pounds was conducted by means of temperature
scanning stress relaxation (TSSR) analysis, as relax-
ation modulus-temperature relations depicted in
Figure 8. Hence, assessing the thermo-elastic prop-
erty at constant strain reveals the modulus-tempera-
ture relationship, as depicted in Figure 8. It is evident
that a slight increase occurs within a narrow temper-
ature range in the initial moduli. The slope and extent

Figure 7. $\tan\delta$ -strain amplitude relationships for ENR-50
compounded with varying concentrations of $ZnCl_2$
at 3, 5, 7, 9, and 12 mmol.
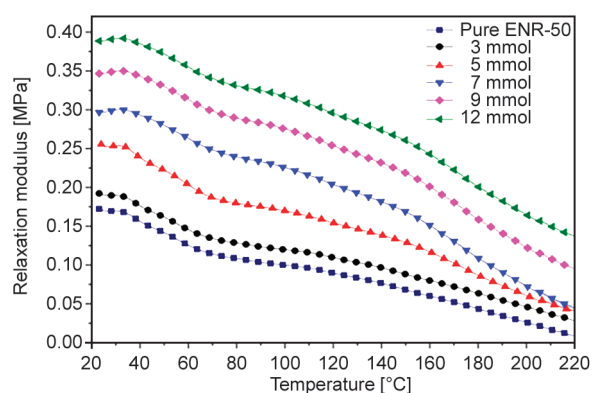
Figure 8. Relaxation modulus-temperature relationship of
ENR-$ZnCl_2$ compounds at various $ZnCl_2$ concen-
trations (3, 5, 7, 9, and 12 mmol) compared to pure
ENR-50.

of this curve are closely linked to the crosslink density of rubber vulcanizates [48]. This appears to be positively correlated with the rising concentration of $ZnCl_2$ in ENR-$ZnCl_2$ compounds. Beyond this temperature range, the relaxation moduli decrease as temperature rises, attributed to the softening effect caused by increased mobility within the rubbery networks at higher temperatures.

Furthermore, this decreasing trend relates to physical or chemical-induced structural changes in the materials. Physical relaxation processes include segmental motions along with disentanglements of chain molecules and other reversible structural changes. On the other hand, chemical relaxation processes are caused by the cleavage of crosslinks or scission of polymer chains, leading to irreversible structural changes [44]. This trend persists until certain intermolecular forces start to weaken, eventually resulting in the breakdown of the crosslink structure and the polymer backbone [49]. As a consequence, the rubber sample ultimately fails at the final test temperature.

Comparison among different types of ENR-$ZnCl_2$ compounds reveals that pure ENR-50 exhibits the lowest relaxation-temperature curve. However, with the incorporation and increasing concentration of $ZnCl_2$, a noticeable rise in these curves is observed. This increase can be attributed to the crosslinking reaction of ENR, facilitated by coordination and internal polymerization, which intensifies as $ZnCl_2$ concentration increases. Consequently, stronger rubbery networks form, leading to higher heat resistance and improved performance under stress relaxation conditions. This correlates well to strength properties (Table 2), crosslink density (Figure 5), and storage moduli (Figure 6).

The thermo-mechanical characteristics of ENR-$ZnCl_2$ compounds were further analyzed using T_{50} and the rubber index (RI). It is noted that T_{50} indicates the relaxation temperature at which the force decreases by approximately 50% compared to the original force. It has been used as the upper limit of the service temperature range [50] alongside compression set resistance [51]. Furthermore, the rubber index (RI) has been used to indicate the elastomeric nature of the material, determined from the area under the normalized force–temperature curve [51]. These results are shown in Figure 9. It is evident that T_{50}, or the upper limit of the service temperature range [50], shows an increasing trend with higher
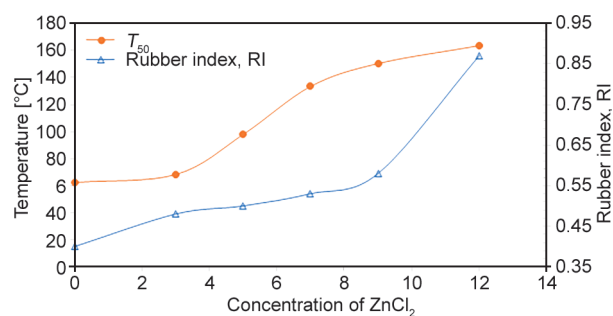
Figure 9. Rubber index (RI) and T_{50} of ENR-$ZnCl_2$ compounds at various $ZnCl_2$ concentrations (3, 5, 7, 9, and 12 mmol) compared to pure ENR-50.

concentrations of $ZnCl_2$. This corresponds to the increasing trend of the rubber index (RI). This suggests that the upper limit of the service temperature range, as well as the elastomeric nature (indicating increased thermal resistance and a superior loss tangent, as shown in Figure 7), is higher for the ENR-$ZnCl_2$ compound with higher $ZnCl_2$ concentration. This is due to enhanced crosslinking reactions (based on reactions depicted in Figure 3), increased crosslink density (Figure 5), and a higher storage modulus during shear deformation at different strain amplitudes (Figure 6).

3.5. Thermal properties

Two distinct methodologies were employed to explore the thermal properties and stability of ENR-$ZnCl_2$ compounds: dynamic mechanical analysis (DMA) and thermogravimetric analysis (TGA). Figure 10 depicts DMA thermograms illustrating the storage modulus (E') and loss tangent ($\tan\delta$) as functions of temperature for ENR-50 compounded with varying $ZnCl_2$ concentrations of 3, 5, 7, 9, and 12 mmol. It is evident that higher storage moduli in the glassy region are observed with increasing $ZnCl_2$ concentration in ENR compounds compared with pure ENR-50 without the addition of $ZnCl_2$. This is likely due to the formation of a stronger rubber network based on coordination (as depicted in Figure 3) and internal polymerization, resulting in an increased crosslink density (as shown in Figure 5). In Figure 10a, as the temperature increases towards the glass transition region, a clear and abrupt decrease in moduli can be observed, indicating the onset of the glass transition temperature (T_g) of the materials. Therefore, the glass transition temperature (T_g) of various materials can be assessed within this temperature range by examining the peak of the $\tan\delta$-temperature relationship, as depicted in Figure 10b, as summarized in
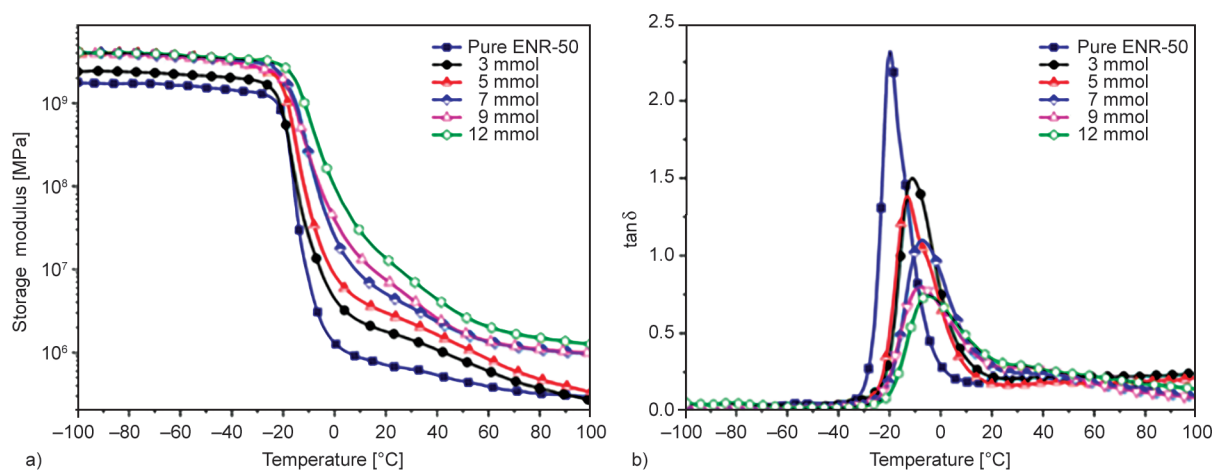
Figure 10. Storage modulus-temperature (a) and tan δ-temperature (b) plots for ENR-50 compounded with various concentrations of ZnCl$_2$ at 3, 5, 7, 9 and 12 mmol.

Table 3. From the thermal analysis, it appears that the glass transition temperatures (T_g) of ENR-ZnCl$_2$ compounds are higher than that of pure ENR-50, indicating greater mobility restriction due to the presence of stronger network structures in the rubber structure. Additionally, a slight increasing trend in T_g is observed with increasing ZnCl$_2$ concentration in the coordination reaction, resulting in a stronger and more rigid rubber vulcanizate, consistent with the stiffness (Figure 4) and hardness (Table 2). In Table 3, the glass transition temperatures (T_g) of all ENR compounds are lower than the freezing temperature, reflecting their elastomeric nature.

In Figure 10a, increasing the test temperature beyond the glass transition region causes a further decreasing trend in storage moduli, albeit at lower gradients, thus forming the rubbery and rubbery flow regions. Furthermore, the final storage modulus at 100 °C increases according to the content of ZnCl$_2$ utilized in the curing reaction.

The thermal stability and resistance of ENR-ZnCl$_2$ compounds with various ZnCl$_2$ concentrations were investigated using the TGA technique, as shown in the TGA and derivative thermogravimetry (DTG) thermograms in Figure 11. The TGA thermograms in Figure 11a exhibit a single degradation stage, occurring between 360 and 450 °C, corresponding to the peaks in the DTG curves shown in Figure 11b. The degradation temperatures (T_ds) of different ENR-ZnCl$_2$ compounds are summarized in Table 3. This degradation stage is attributed to the deterioration of the hydrocarbon content within ENR molecules. Table 3 clearly indicates that the degradation temperature increases with decreasing weight loss, resulting in higher thermal resistance in the ENR compounds with the incorporation and increasing concentrations of ZnCl$_2$. This enhancement in thermal resistance is due to the formation of stronger crosslinking networks via coordination reactions (Figure 3) and internal polymerization, containing
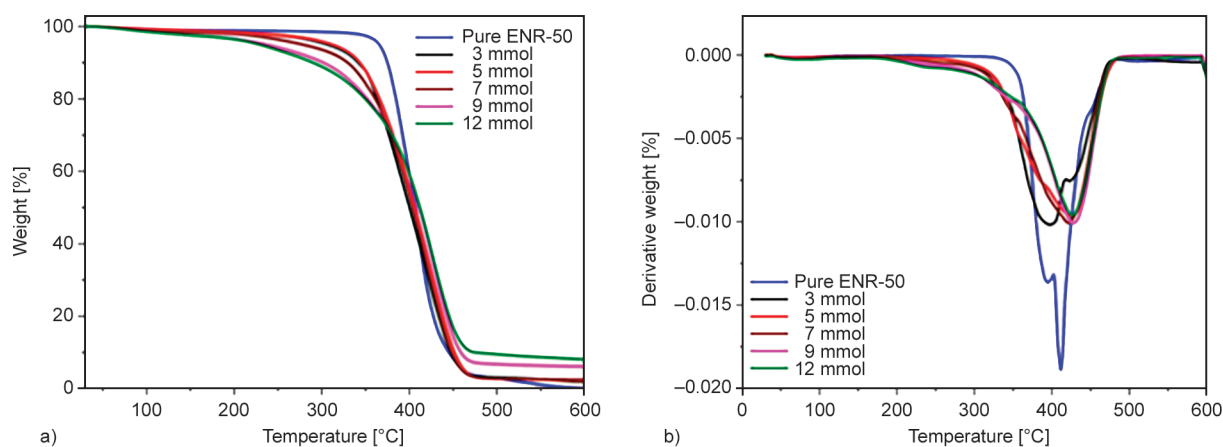
Figure 11. TGA (a) and DTG (b) thermograms of ENR-50 compounded with various concentrations of ZnCl$_2$ at 3, 5, 7, 9, and 12 mmol.

Table 3. Degradation temperature (T_d), glass transition temperature (T_g), as well as percentage weight loss under N_2 atmosphere.

$ZnCl_2$ [mmol]	T_d [°C]	Weight loss [%]	T_g [°C]
Pure ENR 50	390	99.5	−20
3	413	98.4	−19
5	422	98.1	−18
7	422	97.9	−17
9	426	94.2	−17
12	431	92.3	−14

higher contents of high thermal stability –O–Zn–O– linkages in the ENR vulcanizates. These findings are consistent with our previous results from the TGA thermograms of ENR-FeCl$_3$ compounds with –O–Fe–O– linkages [26]. Moreover, these findings are consistent with the thermal resistance observed during the relaxation experiment conducted via a TSSR test, specifically the relaxation modulus-temperature curves (Figure 8) and the T_{50} values (Figure 9), which increase with higher concentrations of $ZnCl_2$, indicating improved thermal stability and thermal resistance.

3.6. Electrical conductivity

Figure 12 illustrates the frequency-dependent electrical conductivity of ENR-$ZnCl_2$ compounds at various concentrations of $ZnCl_2$ (3, 5, 7, 9, and 12 mmol) compared to pure ENR-50. Both pure ENR-50 and ENR-$ZnCl_2$ compounds demonstrate a rising trend in electrical conductivity as the concentration of $ZnCl_2$ increases. This phenomenon can be attributed to the enhancement of electron mobility with increasing frequency of the applied field, consequently elevating the conductivity level [52]. Notably, at a given
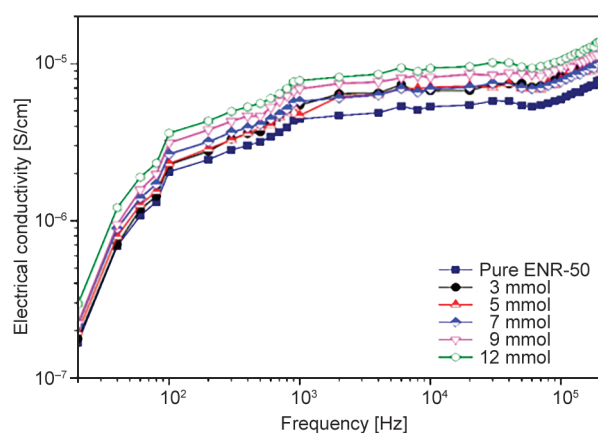
Figure 12. Frequency-dependent electrical conductivity of ENR-$ZnCl_2$ compounds at different concentrations of $ZnCl_2$ (3, 5, 7, 9, and 12 mmol).

frequency, the augmentation of $ZnCl_2$ in ENR compounds leads to an amplified electrical conductivity owing to the increased coordination linkages characterized by –O–Zn–O–, resulting in higher AC conductivity, as depicted in Figure 12. Furthermore, the presence of unreacted $ZnCl_2$ may also contribute to the increase in the electrical conductivity of the ENR-$ZnCl_2$ compounds.

4. Conclusions

ENR-$ZnCl_2$ compounds were prepared with various concentrations of $ZnCl_2$ (1, 3, 5, 7, 9, and 12 mmol) in an internal mixer at 60 °C. The torque response was subsequently assessed using a moving die rheometer (MDR 2000). It was observed that a positive torque response in the sample indicates the occurrence of chemical crosslinks among ENR molecular chains during shear deformation at 160 °C. Subsequently, FT-IR analysis was employed to distinguish the molecular characteristics between ENR-50 and ENR-$ZnCl_2$ compounds. It was observed that the distinct infrared absorption peaks in ENR-$ZnCl_2$ compounds at wavenumbers of 442 and 809 cm^{-1} indicate the presence of –O–Zn–O– coordination bonds linking ENR molecules in the ENR compounds. Additionally, internal polymerization of ENR molecules in the presence of Zn^{2+} ions was also identified. The curing properties of various ENR-$ZnCl_2$ compounds exhibiting a positive torque response were then tested, unveiling a typical curing curve of rubber compounds characterized by slight reversion and a gradual increase in torque with increasing testing time. Increasing concentrations of $ZnCl_2$ resulted in higher minimum and maximum torques and longer cure times but decreased scorch time and cure rate index (*CRI*). Mechanical, dynamic, thermo-mechanical, thermal properties and electrical conductivity were then characterized. The results showed that mechanical properties improved with increasing $ZnCl_2$ concentrations, evidenced by enhanced tensile strength, Young's moduli (stiffness), moduli at 100% elongation, and toughness (from the area under stress-strain curves), as well as increased hardness. This improvement is attributed to increased coordination and internal polymerization reactions, leading to a higher crosslink density of the ENR vulcanizates. However, the ultimate elongation at break tended to decrease due to the stronger crosslinking network. Dynamic mechanical tests confirmed the enhancement of dynamic shear moduli, reflecting the elastic response

of the material and correlating with the improved strength properties. Additionally, decreasing loss tangent (tan δ) values indicated an increasing trend of rubber elasticity. In thermo-mechanical characterization by TSSR tests, the initial moduli and the level of relaxation modulus-temperature curves increased with higher concentrations of $ZnCl_2$ due to intensified coordination and internal polymerization reactions and increased crosslink density. This correlated with an increased rubber index (RI) and enhanced thermal resistance, as indicated by rising T_{50} values. Thermal property characterization of ENR compounds using DMA showed a slight increase in glass transition temperature (T_g) with higher $ZnCl_2$ concentrations due to molecular restriction from stronger crosslinking networks. TGA analysis revealed enhanced thermal stability of ENR-$ZnCl_2$ compounds, with higher degradation temperatures and reduced weight loss. Furthermore, increasing $ZnCl_2$ concentrations also improved the electrical conductivity of the ENR compounds. Therefore, this crosslinking system can be an alternative type of crosslinking agent for ENR in future applications.

Acknowledgements

References

[1] Matchawet S., Kaesaman A., Bomlai P., Nakason C.: Electrical, dielectric, and dynamic mechanical properties of conductive carbon black/epoxidized natural rubber composites. Journal of Composite Materials, **50**, 2191–2202 (2015).
https://doi.org/10.1177/0021998315602941

[2] van Beilen J. B., Poirier Y.: Establishment of new crops for the production of natural rubber. Trends in Biotechnology, **25**, 522–529 (2007).
https://doi.org/10.1016/j.tibtech.2007.08.009

[3] Ngudsuntear K., Limtrakul S., Vatanatham T., Arayapranee W.: Mechanical and aging properties of hydrogenated epoxidized natural rubber and its lifetime prediction. ACS Omega, **41**, 36448–36456 (2022).
https://doi.org/10.1021/acsomega.2c04225

[4] Nakason C., Sasdipan K., Kaesaman A.: Novel natural rubber-*g*-*N*-(4-hydroxyphenyl)maleimide: Synthesis and its preliminary blending products with polypropylene. Iranian Polymer Journal, **23**, 1–12 (2014).
https://doi.org/10.1007/s13726-013-0194-7

[5] Wissamitanan T., Dechwayukul C., Kalkornsurapranee E., Thongruang W.: Proper blends of biodegradable polycaprolactone and natural rubber for 3D printing. Polymers, **12**, 2416 (2020).
https://doi.org/10.3390/polym12102416

[6] Tanrattanakul V., Wattanathai B., Tiangjunya A., Muhamud P.: *In situ* epoxidized natural rubber: Improved oil resistance of natural rubber. Journal of Applied Polymer Science, **90**, 261–269 (2003).
https://doi.org/10.1002/app.12706

[7] Raju A. T., Dash B., Dey P., Nair S., Naskar K.: Evaluation of air permeability characteristics on the hybridization of carbon black with graphene nanoplatelets in bromobutyl rubber/epoxidized natural rubber composites for inner-liner applications. Polymers for Advanced Technologies, **31**, 2390–2402 (2020).
https://doi.org/10.1002/pat.4958

[8] Harun F., Chan C. H.: Electronic applications of polymer electrolytes of epoxidized natural rubber and its composites. in 'Flexible and stretchable electronic composites' (eds.: Ponnamma D., Sadasivuni K., Wan C., Thomas S., Al-Ali AlMa'adeed M.) Springer, Cham, 37–59 (2016).
https://doi.org/10.1007/978-3-319-23663-6_2

[9] Kruželák J., Sýkora R., Hudec I.: Vulcanization of rubber compounds with peroxide curing systems. Rubber Chemistry and Technology, **90**, 60–88 (2017).
https://doi.org/10.5254/rct.16.83758

[10] Kruželák J., Sýkora R., Hudec I.: Sulfur and peroxide curing of rubber compounds based on NR and NBR. Part I: Cross-linking and physical-mechanical properties. KGK Kautschuk Gummi Kunststoffe, **70**, 27–33 (2017).

[11] Suteewong T., Tangboriboonrat P.: Particle morphology of epoxidised natural rubber latex prevulcanized by peroxide system. e-Polymers, **121**, no. 121 (2007).
https://doi.org/10.1515/epoly.2007.7.1.1409

[12] Amran U. A., Zakaria S., Chia C. H.: Epoxidized natural rubber toughened aqueous resole type liquefied EFB resin: Physical and chemical characterization. AIP Conference Proceedings, **1571**, 158–162 (2013).
https://doi.org/10.1063/1.4858647

[13] Pire M., Norvez S., Iliopoulos I., le Rossignol B., Leibler L.: Dicarboxylic acids may compete with standard vulcanisation processes for crosslinking epoxidised natural rubber. Composite Interfaces, **21**, 45–50 (2014).
https://doi.org/10.1080/15685543.2013.830527

[14] Mandal S., Hait S., Simon F., Ghosh A., Scheler U., Arief I., Tada T., Hoang T. X., Wießner S., Heinrich G., Das A.: Transformation of epoxidized natural rubber into ionomers by grafting of 1H-imidazolium ion and development of a dynamic reversible network. ACS Applied Polymer Materials, **4**, 6612–6622 (2022).
https://doi.org/10.1021/acsapm.2c00976

[15] Coran A. Y.: Vulcanization. in 'The science and technology of rubber' (eds.: James E. Mark J. E., Erman B., Roland, C. M.) Academic Press, Cambridge, 337–381 (2013).
https://doi.org/10.1016/B978-0-12-394584-6.00007-8

[16] Hendrikse K. G., McGill W. J.: Vulcanization of chlorobutyl rubber. II. A revised cationic mechanism of $ZnO/ZnCl_2$ initiated crosslinking. Journal of Applied Polymer Science, **78**, 2302–2310 (2000).
https://doi.org/10.1002/1097-4628(20001220)78:13<2302::AID-APP70>3.0.CO;2-B

[17] Ibarra L., Alzorriz M.: Ionic elastomers based on carboxylated nitrile rubber and magnesium oxide. Journal of Applied Polymer Science, **103**, 1894–1899 (2007).
https://doi.org/10.1002/app.25411

[18] Iacob B-C., Bodoki A. E., Oprean L., Bodoki E.: Metal–ligand interactions in molecular imprinting. in 'Ligand' (eds.: Saravanan C., Biswas B.) InTech, London, 3–28 (2018).
https://doi.org/10.5772/intechopen.73407

[19] Shen F., Yuan X., Wu C.: Effects of $SC\text{-}CO_2$ treatment on the properties of $NBR/CuSO_4$ composites. Journal of Macromolecular Science Part B, **47**, 250–259 (2008).
https://doi.org/10.1080/00222340701748586

[20] Mou H., Shen F., Shi Q., Liu Y., Wu C., Guo W.: A novel nitrile butadiene rubber/zinc chloride composite: Coordination reaction and miscibility. European Polymer Journal, **48**, 857–865 (2012).
https://doi.org/10.1016/j.eurpolymj.2012.02.004

[21] Mou H., Xue P., Shi Q., Guo W., Wu C., Fu X.: A direct method for the vulcanization of acrylate rubber through *in situ* coordination crosslinking. Polymer Journal, **44**, 1064–1069 (2012).
https://doi.org/10.1038/pj.2012.59

[22] Ibarra L., Rodríguez A., Mora-Barrantes I.: Crosslinking of carboxylated nitrile rubber (XNBR) induced by coordination with anhydrous copper sulfate. Polymer International, **58**, 218–226 (2009).
https://doi.org/10.1002/pi.2519

[23] Das M., Pal S., Naskar K.: Exploring various metal-ligand coordination bond formation in elastomers: Mechanical performance and self-healing behavior. Express Polymer Letters, **14**, 860–880 (2020).
https://doi.org/10.3144/expresspolymlett.2020.71

[24] Hamzah R., Bakar M. A.: The structural studies of oxirane ring opening reaction in epoxidized natural rubber (ENR-50) by $SnCl_2 \cdot 2H_2O$ and the formation of ENR/TiN complex hybrid. Advanced Materials Research, **626**, 727–737 (2012).
https://doi.org/10.4028/www.scientific.net/AMR.626.727

[25] Zhang X., Tang Z., Guo B., Zhang L.: Enabling design of advanced elastomer with bioinspired metal-oxygen coordination. ACS Applied Materials and Interfaces, **8**, 32520–32527 (2016).
https://doi.org/10.1021/acsami.6b10881

[26] Damampai K., Pichaiyut S., Mandal S., Wießner S., Das A., Nakason C.: Internal polymerization of epoxy group of epoxidized natural rubber by ferric chloride and formation of strong network structure. Polymers, **13**, 4145 (2021).
https://doi.org/10.3390/polym13234145

[27] Damampai K., Pichaiyut S., Das A., Nakason C.: Internal polymerization of epoxy group of epoxidized natural rubber by ferric chloride filled with carbon nanotubes: Mechanical, morphological, thermal and electrical properties of rubber vulcanizates. Express Polymer Letters, **16**, 812–826 (2022).
https://doi.org/10.3144/expresspolymlett.2022.60

[28] Damampai K., Pichaiyut S., Stöckelhuber K. W., Das A., Nakason C.: Ferric ions crosslinked epoxidized natural rubber filled with carbon nanotubes and conductive carbon black hybrid fillers. Polymers, **14**, 4392 (2022).
https://doi.org/10.3390/polym14204392

[29] Buaksuntear K., Panmanee K., Wongphul K., Lim-arun K., Jansinak S., Shah D. U., Smitthipong W.: Enhancing mechanical properties and stabilising the structure of epoxide natural rubber using non-covalent interactions: Metal–ligand coordination and hydrogen bonding. Polymer, **291**, 126626 (2024).
https://doi.org/10.1016/j.polymer.2023.126626

[30] Gong Z., Huang J., Cao L., Xu C., Chen Y.: Self-healing epoxidized natural rubber with ionic/coordination crosslinks. Materials Chemistry and Physics, **285**, 126063 (2022).
https://doi.org/10.1016/j.matchemphys.2022.126063

[31] Tian X., Hu J., Sun X., Duan Y., Jiang M.: Novel application of Zn-containing zeolitic imidazolate frameworks in promoting the vulcanization and mechanical properties of natural rubber composites. Journal of Applied Polymer Science, **140**, e54294 (2023).
https://doi.org/10.1002/app.54294

[32] Flory P. J., Rehner J.: Statistical mechanics of crosslinked polymer networks II. Swelling. The Journal of Chemical Physics, **11**, 521–526 (1943).
https://doi.org/10.1063/1.1723792

[33] Orwoll R. A., Arnold P. A.: Polymer–solvent interaction parameter χ. in 'Physical properties of polymers handbook' (ed.: Mark J. E.) Springer, New York, 233–257 (2007).
https://doi.org/10.1007/978-0-387-69002-5_14

[34] Wu M., Heinz M., Venneman N.: Investigation of unvulcanized natural rubber by means of temperature scanning stress relaxation measurements. Advanced Materials Research, **718–720**, 117–123 (2013).
https://doi.org/10.4028/www.scientific.net/AMR.718-720.117

[35] Siriwas T., Pichaiyut S., Susoff M., Petersen S., Nakason C.: Optimizing the thermomechanical and thermal performance of epoxidized natural rubber hybrid nanocomposites using graphene and carbon nanotubes. Journal of Polymer Research, **31**, 118 (2024).
https://doi.org/10.1007/s10965-024-03962-0

[36] Du F., Fischer J. E., Winey K. I.: Coagulation method for preparing single-walled carbon nanotube/poly(methyl methacrylate) composites and their modulus, electrical conductivity, and thermal stability. Journal of Polymer Science Part B: Polymer Physics, **41**, 3333–3338 (2003).
https://doi.org/10.1002/polb.10701

[37] Nakaramontri Y., Kummerlöwe C., Nakason C., Vennemann N.: The effect of surface functionalization of carbon nanotubes on properties of natural rubber/carbon nanotube composites. Polymer Composites, **36**, 2113–2122 (2015).
https://doi.org/10.1002/pc.23122

[38] Lopes F. L. P., Kupfer V. L., de Oliveira J. C. D., Radovanovic E., Rinaldi A. W., Moisés M. P., Favaro S. L.: Influence of addition of silanized nanosilica and glycerol on hydrophobicity of starch using a factorial design. Polímeros, **27**, 213–219 (2017).
https://doi.org/10.1590/0104-1428.04116

[39] Hitkari G., Singh S., Pandey G.: Structural, optical and photocatalytic study of ZnO and ZnO–ZnS synthesized by chemical method. Nano-Structures and Nano-Objects, **12**, 1–9 (2017).
https://doi.org/10.1016/j.nanoso.2017.08.007

[40] Wang H., Liu W., Huang J., Yang D., Qiu X.: Bioinspired engineering towards tailoring advanced lignin/rubber elastomers. Polymers, **10**, 1033 (2018).
https://doi.org/10.3390/polym10091033

[41] De Lorenzi A., Giorgianni S., Bini R.: High-resolution FTIR spectroscopy of the C–Cl stretching mode of vinyl chloride. Molecular Physics, **96**, 101–108 (1999).
https://doi.org/10.1080/00268979909482942

[42] Arjunan V., Mohan S.: Fourier transform infrared and FT-Raman spectral analysis and *ab initio* calculations for 4-chloro-2-methylaniline and 4-chloro-3-methylaniline. Journal of Molecular Structure, **892**, 289–299 (2008).
https://doi.org/10.1016/j.molstruc.2008.05.053

[43] Dahham O. S., Hamzah R., Bakar M. A., Zulkepli N. N., Dahham S. S., Ting S. S.: NMR study of ring opening reaction of epoxidized natural rubber in presence of potassium hydroxide/isopropanol solution. Polymer Testing, **59**, 55–66 (2017).
https://doi.org/10.1016/j.polymertesting.2017.01.006

[44] Mandal S., Simon F., Banerjee S. S., Tunnicliffe L. B., Nakason C., Das C., Das M., Naskar K., Wiessner S., Heinrich G., Das A.: Controlled release of metal ion cross-linkers and development of self-healable epoxidized natural rubber. ACS Applied Polymer Materials, **3**, 1190–1202 (2021).
https://doi.org/10.1021/acsapm.1c00039

[45] Rufus P., Mohamed N., Shuid A. N.: Cosmos caudatus enhances fracture healing in ovariectomised rats: A preliminary biomechanical evaluation. International Journal of Applied Research in Natural Products, **8**, 12–19 (2015).

[46] Özkaya N., Leger D., Goldsheyder D., Nordin M.: Stress and strain. in 'Fundamentals of biomechanics' (eds.: Özkaya N., Leger D., Goldsheyder D., Nordin M.). Springer, Cham, 287–315 (2017).
https://doi.org/10.1007/978-3-319-44738-4_13

[47] Osoka E., Onukwuli O. D.: Determination of mechanical properties from stress-strain data: A new approach. International Journal of Engineering Research and Advanced Development, **4**, 61–70 (2018).

[48] Blume A., Kiesewetter J.: Determination of the cross-link density of tire tread compounds by different analytical methods. KGK Kautschuk Gummi Kunststoffe, **72**, 33–42 (2019).

[49] Hayeemasae N., Masa A.: Relationship between stress relaxation behavior and thermal stability of natural rubber vulcanizates. Polímeros, **30**, e2020016 (2020).
https://doi.org/10.1590/0104-1428.03120

[50] Pongdong W., Kummerlöwe C., Vennemann N., Thitithammawong A., Nakason C.: A comparative investigation of rice husk ash and siliceous earth as reinforcing fillers in dynamically cured blends of epoxidized natural rubber (ENR) and thermoplastic polyurethane (TPU). Journal of Polymers and the Environment, **26**, 1145–1159 (2018).
https://doi.org/10.1007/s10924-017-1022-5

[51] Kalkornsurapranee E., Keereerak A., Lehman N., Tuljittraporn A., Johns J., Uthaipan N.: Thermo-responsive shape memory thermoplastic elastomer based on natural rubber and ethylene octene copolymer blends. Advances in Polymer Technology, **2023**, 7276854 (2023).
https://doi.org/10.1155/2023/7276854

[52] Jebli M., Rayssi Ch., Dhahri J., Henda M. B., Belmabrouk H., Bajahzar A.: Structural and morphological studies, and temperature/frequency dependence of electrical conductivity of $Ba_{0.97}La_{0.02}Ti_{1-x}Nb_{4x/5}O_3$ perovskite ceramics. RSC Advances, **11**, 23664–23678 (2021).
https://doi.org/10.1039/D1RA01763B